THE JOURNAL OF BIOLOGICAL CHEMISTRY VOL. 286, NO. 6, pp. 4703–4717, February 11, 2011

Stable IgG-like Bispecific Antibodies Directed toward the Type I Insulin-like Growth Factor Receptor Demonstrate Enhanced Ligand Blockade and Anti-tumor Activity[S]

Received for publication, September 12, 2010, and in revised form, November 2, 2010 Published, JBC Papers in Press, December 1, 2010, DOI 10.1074/jbc.M110.184317

Jianying Dong[1], Arlene Sereno, William B. Snyder, Brian R. Miller, Susan Tamraz, Adam Doern, Michael Favis, Xiufeng Wu, Hon Tran, Emma Langley, Ingrid Joseph, Antonio Boccia, Rebecca Kelly, Kathleen Wortham, Qin Wang, Lisa Berquist, Flora Huang, Sharon X. Gao, Ying Zhang, Alexey Lugovskoy, Shelly Martin, Heather Gouvis, Steven Berkowitz, Gisela Chiang, Mitchell Reff, Scott M. Glaser, Kandasamy Hariharan, and Stephen J. Demarest[2]

From Biogen Idec, San Diego, California 92122

Bispecific antibodies (BsAbs) target multiple epitopes on the same molecular target or different targets. Although interest in BsAbs has persisted for decades, production of stable and active BsAbs has hindered their clinical evaluation. Here, we describe the production and characterization of tetravalent IgG-like BsAbs that combine the activities of allosteric and competitive inhibitors of the type-I insulin-like growth factor receptor (IGF-1R). The BsAbs, which were engineered for thermal stability, express well, demonstrate favorable biophysical properties, and recognize both epitopes on IGF-1R. Only one BsAb with a unique geometry, denoted BIIB4-5scFv, was capable of engaging all four of its binding arms simultaneously. All the BsAbs (especially BIIB4-5scFv) demonstrated enhanced ligand blocking over the single monoclonal antibodies (mAbs), particularly at high ligand concentrations. The pharmacokinetic profiles of two IgG-like BsAbs were tested in nude mice and shown to be comparable with that of the parental mAbs. The BsAbs, especially BIIB4-5scFv, demonstrated an improved ability to reduce the growth of multiple tumor cell lines and to inhibit ligand-induced IGF-1R signaling in tumor cells over the parental mAbs. BIIB4-5scFv also led to superior tumor growth inhibition over its parental mAbs *in vivo*. In summary, BsAbs that bridge multiple inhibitory mechanisms against a single target may generally represent a more effective strategy for intervention in oncology or other indications compared with traditional mAb therapy.

Intervening in growth factor pathways has proven to be an effective strategy for treating various cancers. Many growth factor receptors have been successfully targeted using either small molecule or antibody inhibitors or both (1). The type I insulin-like growth factor receptor (IGF-1R)[3] is a member of the insulin receptor tyrosine kinase family. Induction of IGF-1R signaling via its ligands, IGF-1 and IGF-2, has been shown to drive neoplastic cell growth and survival through multiple cellular signaling mechanisms, including the phosphoinositide 3-kinase/Akt pathway (2). Intervention in ligand-dependent IGF-1R signaling was first shown to inhibit tumor cell growth more than two decades ago (3, 4); however, due to the fairly ubiquitous expression of IGF-1R on somatic cells, its known roles in skeletal growth and metabolism, and high homology to the insulin receptor, efforts to clinically develop inhibitors of IGF-1R signaling did not begin in earnest until the turn of the century. Now, several therapeutic monoclonal antibody (mAb) inhibitors and a smaller set of small molecule inhibitors have advanced significantly in the clinic, demonstrating reasonable short-term safety profiles and efficacy in select oncology indications as single agents or in combination with standard-of-care or other approved or investigational agents (5, 6).

The ability to inhibit IGF-1R with mAbs stems from their ability to block ligand-induced signaling as well as a general ability to down-regulate the receptor (5). Many mechanisms of antibody-mediated ligand inhibition have been identified including competitive inhibition of both ligands, partial inhibition of IGF-1, IGF-2, or both by the binding of sites adjacent to the ligand binding site, and allosteric ligand inhibition induced by conformational changes in the receptor that lower ligand affinity (7, 8).

Recently, we have shown that targeting multiple inhibitory epitopes of IGF-1R can result in enhanced ligand blockade, which concomitantly leads to decreased IGF-1R signaling and cell proliferation compared with what could be achieved with single mAbs (9). Positive results of pairing the inhibitory mechanisms of distinct antibodies against single targets for improved activity have been demonstrated in both oncology (10–12) and infectious diseases (13, 14). We tested several antibody combinations against IGF-1R and found that the combination of a purely competitive inhibitor and a purely allosteric inhibitor (8) provided the most compelling activity

[S] The on-line version of this article (available at http://www.jbc.org) contains supplemental Table S1 and Figs. S1–S4.

[1] To whom correspondence may be addressed. Tel.: 858-401-8389; E-mail: jianying_dong@yahoo.com.

[2] To whom correspondence may be addressed: Dept. of Protein Chemistry, Biogen Idec. Tel.: 858-401-5261; Fax: 858-401-5031; E-mail: kdemarest7@gmail.com.

[3] The abbreviations used are: IGF-1R, type I insulin-like growth factor receptor; BsAb, bispecific antibody; $\Delta H_A°(T)$, molar enthalpy of association; $\Delta S_A°(T)$, molar entropy of association; DSC, differential scanning calorimetry; ITC, isothermal titration calorimetry; SEC, size exclusion chromatography; SFM, serum-free medium; SPR, surface plasmon resonance; T_m, midpoint of thermal unfolding transition; PK, pharmacokinetics; BisTris, 2-[bis(2-hydroxyethyl)amino]-2-(hydroxymethyl)propane-1,3-diol.

(9). We hypothesized that converting this antibody combination into a single bispecific antibody (BsAb) might increase the effective concentration of each antigen binding arm upon initial binding to IGF-1R and lead to increased potency. Additionally, generation of a single BsAb that harbors both inhibitory mechanisms may provide a simplified manufacturing and development path.

Interest in BsAbs as novel therapeutics has been strong for decades; however, the practical development of these molecules for clinical use has been hindered by issues with manufacturability as well as by the complexity of bridging multiple biologies or mechanisms of action (15). Early generations of BsAbs involved co-expression of IgGs from different murine species or chemical ligation of different Fabs; of which the former approach has recently yielded the first ever approved BsAb construct (16–18). However, these approaches require complex isolation procedures for manufacturing that may be difficult to scale. Administration of murine-derived BsAbs may also lead to a strong immune response toward the therapeutic in humans. More recently, recombinant technologies have enabled the generation of a much larger variety of BsAbs (19). Depending on the application, some are designed to clear rapidly from circulation to avoid unwanted toxicities, whereas others are designed to have IgG-like serum half-lives as well as potential immune effector functions. Here, we describe IgG-like BsAbs (Fig. 1) directed toward IGF-1R that utilize scFvs appended recombinantly to full-length IgGs to impart bifunctionality, a design that has been described for more than a decade (20). Almost invariably, the generation of recombinant BsAbs involves either removal of antibody variable domains from their native IgG formats or disruption of native protein-protein interfaces within IgGs to facilitate heterodimerization (19, 21). Therefore many engineered antibody formats, including the IgG-like ones described previously, have compromised stability or solubility (22–24). However, new BsAb designs that take into consideration these stability constraints or, as described here, secondarily engineer for protein stability have paved the way for more robust BsAb platforms (25, 26). The stability-engineered BsAbs described here demonstrate improved ligand blocking, improved inhibition of IGF-1R-downstream signaling, and improved inhibition of *in vitro* and *in vivo* tumor cell growth over what we could achieve with single mAbs.

EXPERIMENTAL PROCEDURES

Antibodies, Soluble IGF-1R Receptor, and Ligands—The construction, purification, and characterization of the BIIB4 and BIIB5 mAbs, in-house hIGF-1R(1–903), IGF-1-His tag, and IGF-2-His tag have been described (8). Unlabeled IGF-1 was purchased from R & D Systems. Isotype control antibody C2B8 is a human-mouse chimeric IgG_1 antibody specific to human CD20 from Biogen Idec.

Design of Stable scFvs—The Fv regions of BIIB4 and BIIB5 were constructed as scFvs ($V_L \rightarrow (Gly_4Ser)_4$ linker $\rightarrow V_H$ and $V_L \rightarrow (Gly_4Ser)_3$ linker $\rightarrow V_H$, respectively) and cloned into the pBAD vector (Invitrogen) for constructing expression libraries as described (25, 27). Briefly, scFv libraries were generated by introducing variant codon sequences using the QuikChange II Site-directed Mutagenesis Kit according to the manufacturer's instructions (Stratagene). Polyacrylamide gel electrophoresis-purified oligonucleotides were obtained from Valuegene, Inc. Products of mutagenesis reactions were transformed into *Escherichia coli* strain XL10-GOLD® (Stratagene). Libraries were plated onto LB agar plates containing 50 mg/ml of carbenicillin (Teknova). Pooled plasmid DNA was prepared from the library and used to transform *E. coli* strain W3110 (American Type Culture Collection, ATCC) and prepare arrayed libraries as described (27).

Stabilizing designs that served as the basis for the scFv libraries were generated using both sequence (28, 29) and structure-based methods (30). The expressed libraries were challenged at various temperatures for 1 h prior to assaying scFv activity by DELFIA (27). "Hits" from the thermal challenge screen were re-arrayed and tested in duplicate for T_{50}, the midpoint temperature at which 50% of the scFv activity remains after thermal challenging for 1 h (25). If necessary, multiple hits were combined using the QuikChange II Site-directed Mutagenesis Kit and re-assessed for their T_{50} until an empirical $T_{50} \geq 65$ °C was reached.

Construction of Full-length BsAbs—Construction of mammalian expression vectors for the κ light and IgG1 heavy chains of both BIIB4 and BIIB5 has been described previously (8). Signal peptides for the BsAbs were derived by evaluating the closest sequence matches to other antibody heavy and light chain proteins produced at Biogen Idec and were identical for all constructs. The light chain vectors of the parental antibodies could be recycled for BsAb expression (8). The BsAb heavy chain vectors were constructed from the parental mAb constructs using primers designed to create inserts containing the stabilized BIIB4 or BIIB5 scFv gene sequences (the BIIB4 scFv was recoded for mammalian expression). Subcloning of the only N-terminal BsAb, 5scFv-BIIB4, necessitated the intermediary subcloning of an additional MhuI site into the parental BIIB4 mAb vector following the heavy chain signal sequence. A BIIB5 scFv insert containing a 3′-$(G_4S)_5$ linker codon sequence was then subcloned between the signal and BIIB4 heavy chain sequences of the intermediary BIIB4 plasmid using the engineered MhuI site and an existing NheI site to yield a plasmid encoding the 5scFv-BIIB4 BsAb. The C-terminal BsAbs, BIIB4-5scFv, BIIB5-5scFv, and BIIB5-4scFv were constructed by subcloning the scFv inserts (all containing 5′-$S(G_4S)_3$ linker codon sequences within naturally occurring BamHI and DraIII sites within the parental BIIB4 or BIIB5 plasmids). The ligation mixtures were transformed into TOP 10 *E. coli* competent cells (Invitrogen). *E. coli* colonies transformed to ampicillin drug resistance were screened for the presence of the inserts. DNA sequence analysis was used to confirm the correct sequence of the final constructs encoding all four BsAbs.

Mammalian Cell Expression—Plasmid DNA was used to transfect in-house serum-free adapted DG44-CHO host cells (31) by electroporation using a GenePulser II instrument (Bio-Rad) as described previously (32). Transformants were selected in a proprietary cloning medium (33). After ~14 days in selection, cells were subjected to enrichment followed by cell line isolation in 96-well plates using fluorescence-activated cell sorting

(FACS) (34). For the BIIB4-5scFv BsAb, isolates were further amplified by methotrexate exposure and subcloned by FACS to select the final cell lines. Cells were scaled for bispecific antibody production in 3-liter Applikon bioreactors.

Purification of Bispecific Antibodies—CHO supernatants containing the BsAbs were purified over columns containing mAb Select resin (GE Healthcare) on an AKTA explorer (GE Healthcare). For BIIB5-5scFv and BIIB5-4scFv, it was necessary to perform a second purification step using a size exclusion column (Superdex 200, GE Healthcare) to remove the ~10% aggregates (predominantly protein dimer) that were found in the mAb Select eluants. Where necessary, proteins were concentrated using Amicon stirred cell concentrators (Millipore). The proteins were all dialyzed using Slide-A-Lyzers or SnakeSkin (Thermo Scientific) into a final PBS buffer. Protein quality was analyzed by SDS-PAGE using 4–12% Bis-Tris gels and the Mark 12 protein molecular weight standard (Invitrogen).

Analytical Size Exclusion with In-line Light Scattering—The oligomeric states of the BsAbs and BsAb-IGF-1R complexes were assessed using analytical size exclusion chromatography (SEC) with in-line static light scattering. For each sample, 60 μg of BsAb (or 45 μg of mAb), 30 μg of hIGF-1R(1–903), or a combination of 60 μg of BsAb (or 45 μg mAb) and 30 μg of receptor were injected onto a Biosep-SEC-S3000 analytical SEC HPLC (7.8 × 300 mm) column (Phenomenex) equilibrated in 10 mM phosphate, 150 mM NaCl, 0.02% NaN_3, pH 6.8, using an Agilent 1100 HPLC system. Light scattering data for material eluted from the SEC column were collected using a mini-DAWN static light scattering detector coupled to an in-line refractive index meter (Wyatt Technologies). UV data were analyzed using HPCHEM (Agilent). Molecular weights of the complexes were determined by their static light scattering profiles using ASTRA V (Wyatt Technologies).

Stoichiometric Determination of the Number of BsAb Binding Sites on IGF-1R Using Equilibrium Surface Plasmon Resonance (SPR)—All experiments were performed on a Biacore3000 instrument (Biacore). The BIIB4 and BIIB5 mAbs were separately immobilized to two different flow cell surfaces of a standard CM5 chip surface using standard amine chemistry protocols provided by the manufacturer. At high immobilization levels of mAb (~10,000 resonance units), flowing low concentrations of hIGF-1R(1–903) (<50 nM) led to mass-transfer limited linear binding curves whose initial velocity of binding, V_i (resonance units/s), depended linearly on the concentration of the hIGF-1R(1–903) solution flowed over the chip surface. Binding constants and stoichiometries of binding could be determined by flowing mixtures of hIGF-1R(1–903) and the Fabs, mAbs, or BsAbs over the sensorchip surface containing BIIB4 or BIIB5. The BIIB4 and BIIB5 sensorchip surface measures the concentration of unbound or free hIGF-1R(1–903) ($[R]_F$) in solutions containing hIGF-1R(1–903) and Fab/mAb/BsAb. Unbound IGF-1R(1–903) is equal to the total amount of receptor in solution ($[R]_T$) minus the bound concentration ($[R]_B$). The equilibrium dissociation constant (K_D) and binding stoichiometry (n) between the antibodies and hIGF-1R(1–903) were determined using the linear relationship between $[R]_F$ and V_i using the equation,

$$V_i = m \times \left[[R]_T - \frac{1}{2}\{(n[Ab]_T + [R]_T + K_D) - \sqrt{(n[Ab]_T + [R]_T + K_D)^2 - 4n[Ab]_T[R]_T}\} \right] \quad \text{(Eq. 1)}$$

where m = slope of the hIGF-1R(1–903) concentration-dependent standard curve and $[Ab]_T$ = total Fab/mAb/BsAb concentration (35).

Fluorescence Resonance Energy Transfer (FRET) Assay—BIIB4-5scFv was Europium labeled and mixed with Cy5-labeled sIGF-1R(1–903). The binding of Eu-BIIB4 or Eu-BIIB5 to Cy5-hIGF-1R(1–903) results in a strong time-resolved fluorescence resonance energy transfer from the Europium label to the Cy5 label. Inhibition of the interaction by the binding of unlabeled reagents to the labeled reagents results in a loss of signal. Serial dilutions of unlabeled Fabs, mAbs, and BsAbs starting at 2 μM (50 μl total) were mixed with 25 μl of Cy5-hIGF-1R(1–903)-Cy5 at 1 μg/ml and 25 μl of Eu-BIIB4-5scFv at 2 μg/ml in 96-well microtiter plates (black from Costar). The total volume was 100 μl for each sample. Plates were incubated for 1 h at room temperature on a plate agitator. Fluorescence measurements were carried out on a Wallac Victor^2 fluorescent plate reader (PerkinElmer Life Sciences) using the LANCE protocol with the excitation wavelength at 340 nm and emission wavelength at 665 nm.

Ligand Blocking Assay—The ELISA-based method for measuring the Fab/mAb/BsAb-mediated blockade of IGF-1 and IGF-2 from binding IGF-1R was performed as described previously (8).

Tumor Cell Lines—Non-small cell lung carcinoma cell line NCI-H322M was obtained from the NCI, National Institutes of Health. Non-small cell lung carcinoma cell line A549, osteosarcoma cell line SJSA-1, pancreas adenocarcinoma cell line BxPC3, epidermoid carcinoma cell line A431, and colorectal adenocarcinoma cell line HT-29 were all purchased from the American Type Culture Collection (ATCC). All cells were routinely cultured and maintained in RPMI 1640 medium supplemented with 10% fetal bovine serum (FBS).

IGF-1R Internalization—Western blot analyses of IGF-1R down-regulation were essentially performed as described previously (8) using 100 nM mAb or BsAb. Flow cytometry analyses of IGF-1R down-regulation were also performed as described previously (9) using 100 nM mAb or BsAb.

Signaling Analyses—Measurement of the relative levels of both IGF-1R and Akt phosphorylation in the absence and presence of each mAb or BsAb was performed as described previously for the BIIB4 and BIIB5 combination (9). Briefly, cells were grown in RPMI 1640 medium containing 10% FBS overnight and then serum-starved for 24 h. The cells were treated with 0.1, 1, 10, or 100 nM of control antibody C2B8, BIIB5, BIIB4, BIIB4-5scFv, or a combination of BIIB4 and BIIB5 each at the above indicated concentrations for 1 h before being stimulated with 100 ng/ml of IGF-1 (R & D Systems) for 20 min. Cellular proteins were extracted in a lysis buffer (Cell Signaling Technology). Cellular phospho-IGF-1R (Tyr-1135/1136), IGF-1R, phospho-Akt (Thr-308), Akt, and β-actin proteins were analyzed by Western blot using primary

antibodies from Cell Signaling Technology and a secondary antibody conjugate anti-rabbit IgG-HRP (Jackson ImmunoResearch) followed by development with the SuperSignal Western Substrate Kit (Pierce). Chemiluminescence images were captured and densitometric quantification of protein bands was performed using the VersaDoc 5000 imaging system from Bio-Rad. Phospho-Akt and total Akt levels in cell lysates were also measured using a phospho-Akt (Ser-473)/total Akt duplex Meso Scale Discovery kit following the manufacturer's protocol and the percentage of *p*-Akt over total Akt was calculated according to the manufacturer's recommendation using the formula: $(2 \times p\text{-Akt})/(p\text{-Akt} + \text{Akt}) \times 100)$.

Cell Growth Inhibition Assay—Tumor cells were seeded at 5000–8000 cells per well in 96-well plates and grown overnight. Then cells were treated with BIIB4, BIIB5, or the individual BsAbs in serum-free medium (SFM) or 10% FBS-containing medium supplemented with IGF-1 and/or IGF-2. After 3 days, cell viability was determined with a Cell Titer Glo reagent (Promega) per the manufacturer's instructions. The percentage of growth inhibition under serum-free conditions was calculated according to the formula [1 − (signal with inhibitor (mAb or BsAb) − signal in SFM)/(signal with IGF − signal in SFM)] × 100, whereas in the presence of serum it was calculated according to the formula [1 − (signal with inhibitor/signal with IGF)] × 100).

Cell Cycle Analysis—SJSA-1 cells were seeded at 2×10^5 cells/well into 6-well plates and cultured overnight in RPMI 1640 medium containing 5% FBS. Then cells were serum-starved for 24 h before treatment with 100 ng/ml of both IGF-1 and IGF-2 in the presence of 100 nM C2B8, BIIB5, BIIB4, and the BIIB5/BIIB4 combination, or BIIB4-5scFv for 48 h. Cells were fixed in pre-chilled 70% ethanol and stained with propidium iodide (20 μg/ml) for 30 min at room temperature before FACS analysis of DNA contents. The relative percentage of cells in the G_0/G_1, S, and G_2/M phase were calculated from histograms using the FlowJo 7.7.2 software.

Soft-agar Colony Formation Assay—A layer of 0.6% agar prepared with RPMI 1640 supplemented 10% FBS was poured into 24-well culture plates and allowed to solidify. Then, SJSA-1 cells mixed with 0.3% agar in medium containing 100 nM of the C2B8 IgG1 control, BIIB4, BIIB5, the BIIB4/BIIB5 combination (each at 50 nM), or BIIB4-5scFv in the absence or presence of 100 ng/ml of both IGF-1 and IGF-2 were plated at 2000 cells/well on top of the 0.6% agar layer. The plates were incubated at 37 °C in a 5% CO_2 incubator for 5 weeks, and colonies above 10 μm were counted with an automated mammalian cell colony counter (Oxford Optronix GELCOUNT).

Pharmacokinetics (PK) of BIIB4-5scFv and 5scFv-BIIB4 in Mice—Mice were maintained in accordance with the Biogen Idec Institutional Animal Care and Use Committee and city, state, and federal guidelines for the humane treatment and care of laboratory animals. A single dose PK study was conducted with the BsAbs in female nude mice (8—10 weeks old, Charles River Laboratories). The mice were dosed intraperitoneally with 10 mg/kg of BIIB4, BIIB5, BIIB4-5scFv, or 5scFv-BIIB4. At various time points post dosing, mice were sacrificed, and blood was collected by cardiac puncture and separated for serum recovery. Time points included pre-dosing, post-dosing at 0.25, 0.5, 1, 2, 6, and 24 h, and at 2, 4, 7, 9, 11, and 14 days post-dosing. Serum samples were frozen at the time of collection and later tested by ELISA for the presence of antibodies.

Briefly, ELISA plates were coated with goat anti-human IgG (Southern Biotech) overnight at 4 °C and then blocked with 1% nonfat milk and 0.05% Tween 20 in PBS at room temperature for 1 h. Serial dilutions of sample serum were added to the coated plates and incubated for 1 h, followed by an additional incubation with detection antibody (goat anti-human κ-HRP, Southern Biotech) for 1 h at room temperature. Test articles (BIIB4, BIIB5, BIIB4-5scFv, and 5scFv-BIIB4) of known concentrations were serially diluted 1:25 in normal mouse serum (Chemicon) and included in the assay to generate standard curves. Washes were performed between incubations. The plate was developed by the addition of TMB substrate (3.3′,5.5′-tetramethylbenzidine, Kirkegaard & Perry Labs), and the reaction was stopped with H_2SO_4. OD (optical density) at 450 nm of each well was measured using a microplate reader (SpectraMax M2, Molecular Devices). The data were analyzed using SoftMax Pro, and concentrations of the human mAbs and BsAbs in mouse serum were determined from the standard curves. Pharmacokinetic properties were calculated using the noncompartmental module of WinNonLin (Pharsight).

Tumor Xenograft Study—All animal studies were conducted under conditions and protocols approved by the Institutional Animal Care and Use Committee. The SJSA-1 osteosarcoma xenografts were established in nude mice (8—10 weeks old, Charles River Laboratories) by injecting subcutaneously 5×10^6 cells in 20% Matrigel in the flank region. When tumors reached an average volume of 180 mm^3 on day 20, the mice with tumors were randomly sorted into 5 groups ($n = 10$). Mice were treated intraperitoneally with equal molar doses of BIIB5 (7.5 mg/kg), BIIB4 (7.5 mg/kg), BIIB4-5scFv (10 mg/kg), 5scFv-BIIB4 (10 mg/kg), or the control antibody C2B8 (7.5 mg/kg) once a week for 3 weeks. Tumor measurement was taken twice weekly, and tumor sizes were calculated using the formula: volume = ½ (length × $width^2$). Data plotting and statistical analysis were conducted using the GraphPad Prism software.

RESULTS

Generation of Bispecific and Multivalent Antibodies Directed against IGF-1R—The Fv regions of BIIB4 (competitive IGF inhibitor) and BIIB5 (allosteric IGF inhibitor) (8) were used to create scFvs that serve as building blocks for making BsAbs that recognize both inhibitory epitopes on IGF-1R. Generation of robust IgG-like BsAbs using scFvs as building blocks requires that the scFvs have adequate stability and solubility properties. However, removal of the Fv region from the native context of the Fab region of an antibody routinely leads to a significant drop in the stability of the variable domains (22, 36). Based on a thermostability analysis of a panel of human and humanized antibodies from various commercial, clinical, and preclinical stages of development including some with relatively ideal development characteristics and others

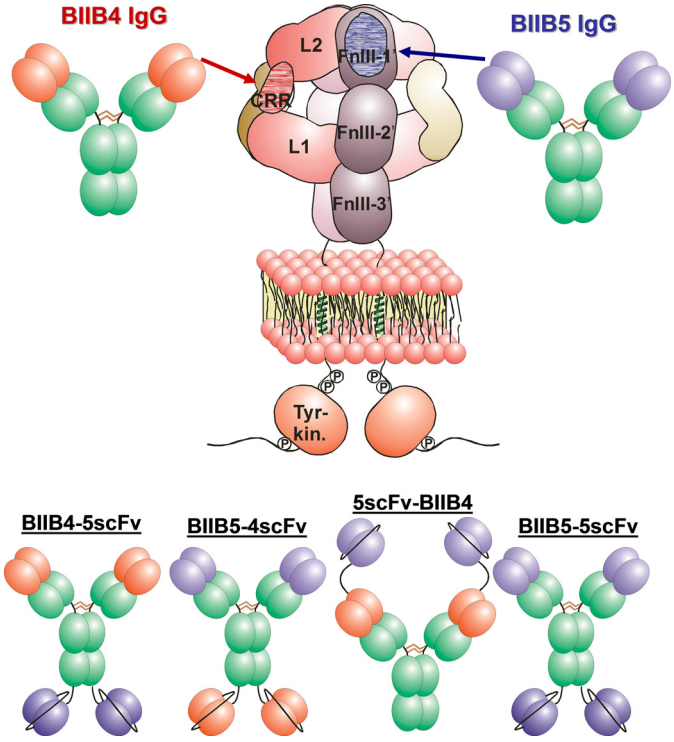

FIGURE 1. **Schematic diagram of IGF-1R, the BIIB4 and BIIB5 mAbs, the various BsAbs (BIIB4-5scFv, 5scFv-BIIB4, BIIB5-4scFv), and tetravalent BIIB5 (BIIB5-5scFv).** The domains of IGF-1R are labeled (from the N terminus): *L1*, 1st receptor L domain; *CRR*, cysteine rich region; *L2*, 2nd receptor L domain; *FnIII-1,2,3*, 1st, 2nd, and 3rd type III fibronectin domains. The putative epitopes of BIIB4 (*red*) and BIIB5 (*blue*) are illustrated on the schematic diagram of IGF-1R.

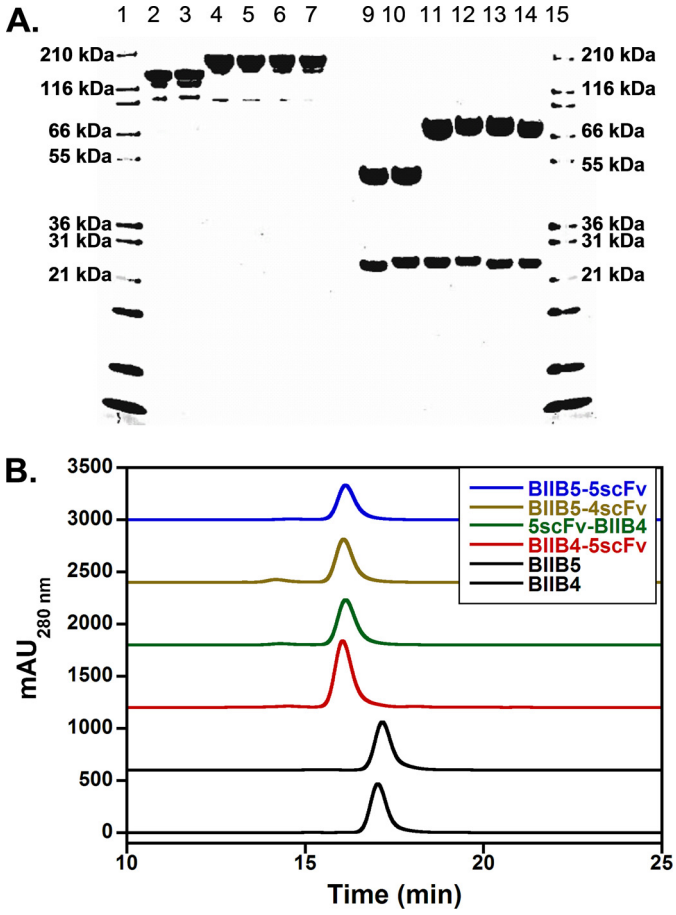

FIGURE 2. **SDS-PAGE analysis and analytical size exclusion chromatography of the BsAbs demonstrate their proper assembly and predominantly monomeric status in solution.** *A*, 4–12% BisTris NuPage gel analysis (from left to right) of BIIB4, BIIB5, BIIB4-5scFv, 5scFv-BIIB4, BIIB5-4scFv, and BIIB5-5scFv. The group on the *left* (*lanes 2–7*) was non-reduced, whereas the group on the *right* (*lanes 9–14*) was reduced with 100 mM DTT. Molecular weight markers are shown in *lanes 1* and *15*. *B*, overlays of analytical size exclusion chromatograms of the six proteins. Each chromatograph represents a 30-μg injection. Static light scattering measurements indicate that all the observable peaks are monomeric (molecular mass ~ 150 kDa for the mAbs and ~200 kDa for the BsAbs).

with clear tendencies toward aggregation and misfolding, we found that mAbs whose Fabs have midpoints of thermal denaturation (T_m) greater than ~65 °C typically are more likely to have reasonable development properties (28). Therefore, we generally set an empirical lower T_m limit of 65 °C for scFvs utilized for BsAbs, which is at the lower limit of apparent thermal stability of IgG Fabs (25, 26). The BIIB4 and BIIB5 scFvs had apparent thermal stabilities below 65 °C using a thermal challenge assay. Potentially stabilizing designs were generated using sequence- and structure-based methods (supplemental Table S1). These designs were screened using the thermal challenge assay (27). The BIIB5 scFv only necessitated a single mutation (V_L I83E) to reach a T_m above 65 °C (supplemental Fig. S1). For the BIIB4 scFv, multiple stabilizing hits (V_L_L50N, V83E, A84G; V_H_E6Q, S49A) were combined until a T_m above 65 °C was reached (supplemental Fig. S1) (25, 27).

In an effort to generate a BsAb with equal or better activity than what was observed with the BIIB4/BIIB5 mAb combination, several BsAb or tetravalent IgG molecules were constructed (Fig. 1). First, we generated two BsAbs with scFvs appended to the C terminus of an antibody; the first having the BIIB4 IgG1 attached via a $(GGGGS)_3$ linker to the stabilized BIIB5 scFv (BIIB4-5scFv) and the second having the BIIB5 IgG1 attached using the same linker to the stabilized BIIB4 scFv (BIIB5-4scFv). Conceptually, this format should allow significant spacing between the antigen binding domains of the IgG and the scFvs. A second format was generated by attaching the BIIB5 scFv to the N terminus of the BIIB4 IgG1 using a $(GGGGS)_5$ linker, bringing the antigen binding moieties of the BsAb into a much closer proximity to one another (5scFv-BIIB4). Last, we built a tetravalent version of the BIIB5 antibody by appending the stabilized BIIB5 scFv to the C terminus of the BIIB5 IgG1 (BIIB5-5scFv). This construct should help discriminate the properties of simply increasing valency from the activity afforded by targeting two inhibitory epitopes.

The different constructs were all well expressed in CHO. The product quality of the material generated by purification of CHO supernatants through protein A chromatography was generally very high as assessed by SDS-PAGE (Fig. 2*A*). Faint bands below the major bands in the non-reduced lanes for both the mAbs and BsAbs are likely the result of low-level reduction of the hinge disulfides by residual unpaired cysteines present throughout the antibody molecule and are commonly observed for antibodies in general (37). BIIB4-5scFv and 5scFv-BIIB4 yielded ~97% monomeric material after this first step, whereas BIIB5-4scFv and BIIB5-5scFv

TABLE 1
Results of DSC and circular dichroism (CD) with inhibitory IGF-1R mAbs, BsAbs, and tetra BIIB5

	scFv T_m[a] (ΔH_{cal}, ΔH_{vH})[b]	C_H2 T_m (ΔH_{cal}, ΔH_{vH})	Fab T_m (ΔH_{cal}, ΔH_{vH})	C_H3 T_m (ΔH_{cal}, ΔH_{vH})
DSC data				
BIIB4 IgG1		71.6 (230, 110)	78.0 (410, 170)	85.0 (90, 240)
BIIB5 IgG1		71.5 (230, 130)	83.0 (720, 180)	84.5 (230, 130)
BIIB4-5scFv	65.9 (370, 100)	71.5 (120, 190)	76.9 (530, 150)	85.1 (100, 200)
5scFv-BIIB4	67.3 (410, 90)	70.6 (110, 170)	76.1 (410, 160)	84.6 (110, 210)
BIIB5-4scFv	66.8 (240, 110)	69.0 (80, 230)	82.5 (550, 150)	84.5 (100, 230)
BIIB5-5scFv	65.8 (380, 120)	70.5 (80, 230)	82.6 (830, 150)	84.5 (90, 250)
CD data	scFv T_m(DH_{vH})			
BIIB4-5scFv	65.3 ± 0.4 (530)	–[c]	–[c]	–[c]
5scFv-BIIB4	67.0 ± 0.5 (-[c])	–[c]	–[c]	–[c]

[a] °C.
[b] kcal/mol.
[c] Obscured by Fab-induced precipitation.

were between 80 and 90% monomeric after this first step. The reason for the observed differences in the purity of the proteins off protein A was not entirely clear. However, all the BsAb/tetravalent proteins could be stably purified to >95% monomer (Fig. 2*B*).

Biophysical Stability and Manufacturability of Bispecific and Tetravalent Antibodies—Instability and solubility issues with engineered proteins such as mAb fragments and BsAbs that contain them have limited their development as therapeutic candidates (22). Thus, it is important in any study proposing the use of highly engineered protein therapeutics to report some assessment of protein stability. Here, the stability of the BsAbs was assessed using several methods. First, all the BsAbs and mAbs could be concentrated in PBS to >5 mg/ml without reaching solubility limits (BIIB4-5scFv has been concentrated to >150 mg/ml in a pre-formulation buffer). Concentrating the BsAbs above 5 mg/ml did not lead to molecular dimerization or higher order aggregates as assessed by size exclusion/static light scattering. This was additionally confirmed for BIIB4-5scFv and 5scFv-BIIB4 using analytical ultracentrifugation (data not shown). We formally investigated the long term stability of both BIIB4-5scFv and 5scFv-BIIB4 in PBS at 10 mg/ml at 4 °C and observed virtually no protein loss or aggregation over extended periods (up to 5 months; supplemental Fig. S2*A* for BIIB4-5scFv) and have not witnessed significant increases in aggregates with BIIB5-4scFv or BIIB5-5scFv while working with stock solutions over a few months. The research (non-amplified) cell lines consistently reached >100 mg/liter expression for the BsAbs (except for BIIB5-5scFv where material was generated using a transfected/sorted CHO cell pool). An amplified cell line was produced for BIIB4-5scFv that reached an expression level of 3.7 g/liter; a level easily suitable for commercial production.

The thermal stability of the scFvs within the multivalent constructs was examined by differential scanning calorimetry (DSC) and in some instances circular dichroism (CD). Similar to what was observed in the thermal challenge assay, DSC confirmed that the T_m of both the BIIB4 and BIIB5 scFvs was above our empirical threshold criteria of 65 °C (supplemental Fig. S2*B* and Table S1). In general, the presence of an appended scFv did not significantly impact the unfolding properties of the other domains of the IgGs (Table 1). Interestingly, both the far and near UV CD spectra of BIIB4-5scFv and 5scFv-BIIB4 show no sign of large aggregate formation or precipitation until the Fab unfolds (supplemental Fig. S2*C* for near UV spectra of BIIB4-5scFv at various temperatures). Previous studies have shown that V_H and C_H1 domains are more prone to expression/aggregation issues than V_L or C_L domains (38, 39). However, the V_H domains of BIIB4 and BIIB5 were derived from a phage display library using a V_H3 subclass domain framework with ideal refolding properties (40). Thus, the precipitation observed for the Fab of the BsAbs was likely the result of C_H1 aggregation with itself or other unfolded domains of the protein.

Multivalent Binding of Bispecific and Tetravalent Antibodies—A difficulty in demonstrating the tetravalent nature of the bispecific antibodies is that all four binding arms recognize a single target, IGF-1R, but not all with the same epitope. Therefore, to measure the binding characteristics of the BsAbs and BIIB5-5scFv, cross-blocking studies with the parental BIIB4 and BIIB5 mAbs were performed. Because BIIB4 and BIIB5 do not cross-block one another, most of the assays developed to assess the tetravalent activity examine stoichiometric blockade of BIIB4 or BIIB5 separately.

First, equilibrium, solution-phase SPR studies were performed to investigate the affinity and stoichiometry of BsAb binding to both the BIIB5 and BIIB4 epitopes. When run under mass-transfer limiting conditions utilizing densely immobilized BIIB4 or BIIB5, the SPR instrument can measure the level of free IGF-1R in solution in the absence or presence of titrating levels of soluble BIIB4 mAb or Fab, BIIB5 mAb or Fab, the various BsAbs, or BIIB5-5scFv (8). To obtain enough signal, 50 nM hIGF-1R(1–903) was used, which limited our ability to accurately measure affinity below 0.5 nM. It should be noted that the hIGF-1R(1–903) protein is a constitutive dimer and theoretically contains two BIIB4 *and* two BIIB5 epitopes.

Competition experiments with hIGF-1R(1–903) binding to the BIIB5 surface clearly demonstrate the bivalent binding of BIIB4-5scFv and BIIB5-4scFv as well as tetravalent binding of BIIB5-5scFv to the BIIB5 epitope (Fig. 3*A*, Table 2). Because hIGF-1R(1–903) is a constitutive dimer, its binding to bivalent mAbs involves a significant avidity factor that increases the apparent affinity of the BIIB5 mAb beyond the lower threshold of detection (K_D < 0.5 nM). The BIIB4 mAb and Fab did not block binding to the BIIB5 surface as expected.

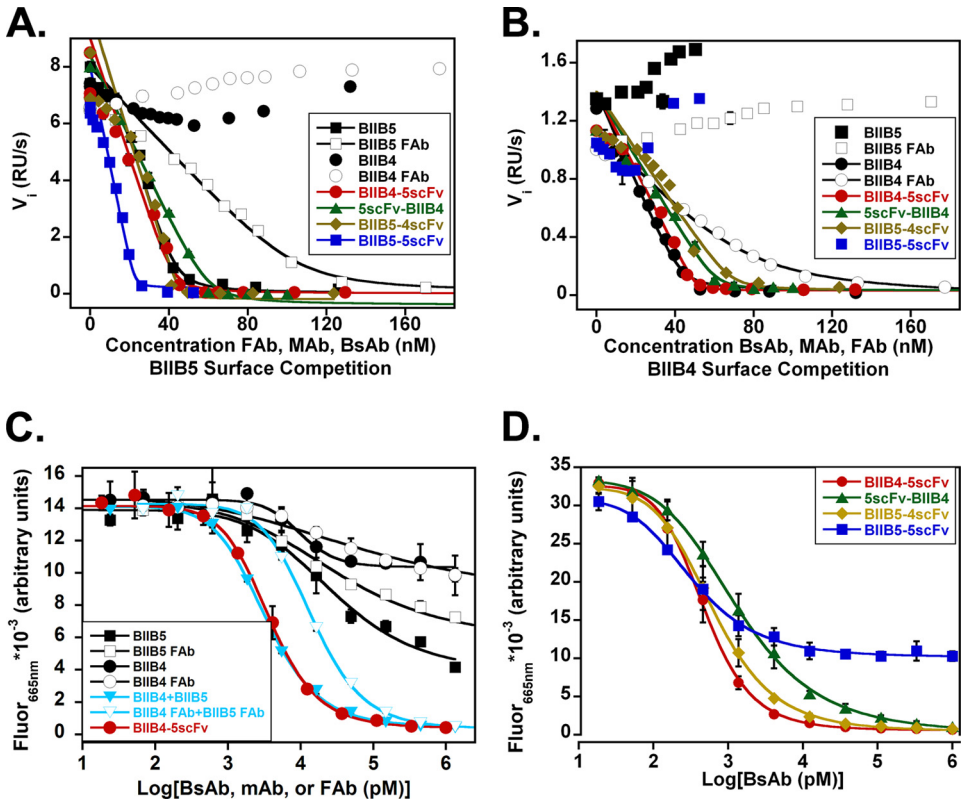

FIGURE 3. **Stoichiometry of binding and saturation of both IGF-1R epitopes.** *A* and *B,* equilibrium binding curves of the mAbs, Fabs, and BsAbs binding to hIGF-1R(1–903). The V_i measurements are the mass transfer-limited signals achieved by the binding of binding of free hIGF-1R(1–903) to a sensorchip surface coated with BIIB5 (*A*) or BIIB4 (*B*). *C* and *D,* inhibition of Eu-BIIB4-5scFv binding to Cy5-hIGF-1R(1–903) using the unlabeled mAbs, Fabs, and BsAbs. All experiments were performed in duplicate and include *visible error bars* only when the error was larger than the data points.

TABLE 2

Results of equilibrium, solution-phase SPR affinity, and stoichiometry of binding measurements with IGF-1R and the various Fabs, mAbs, and BsAbs

Construct	BIIB4 surface		BIIB5 surface	
	K_D	*n* (IGF-1R/Ab)	K_D	*n* (IGF-1R/Ab)
	nM		nM	
BIIB4	0.6 ± 0.1	1.0 ± 0.2		
BIIB4 Fab	4.6 ± 1.0	0.6 ± 0.1		
BIIB5			0.4 ± 0.2	1.1 ± 0.1
BIIB5 Fab			0.9 ± 0.3	0.5 ± 0.1
BIIB5-4scFv	0.3 ± 0.2	0.70 ± 0.10[a]	0.1 ± 0.4	1.1 ± 0.2
BIIB4-5scFv	0.1 ± 0.03	1.0 ± 0.1	0.2 ± 0.2	1.0 ± 0.1
5scFv-BIIB4	0.7 ± 0.4	0.72 ± 0.06[a]	0.2 ± 0.1	0.75 ± 0.05[a]
BIIB5-5scFv			0.2 ± 0.3	2.2 ± 0.3

[a] Deviation from expected stoichiometry based on the number of antigen binding sites on the BsAb construct.

Unlike the other BsAbs, it was necessary to add roughly 25% more 5scFv-BIIB4 than the others to fully titrate hIGF-1R(1–903) (Fig. 3*A*).

Next, the activity of the BsAbs was tested on the BIIB4 surface (Fig. 3*B*, Table 2). As before, BIIB4 mAb and Fab provided good standards for the proper stoichiometry of binding to hIGF-1R(1–903), whereas the BIIB5 mAb and Fab did not compete with the BIIB4 surface. Additionally, BIIB5-5scFv did not compete with the BIIB4 surface because its antigen binding sites are all directed toward the BIIB5 epitope. BIIB4-5scFv blocked the BIIB4 surface similar to the BIIB4 mAb, suggesting no interference between the various binding arms of the BsAb. 5scFv-BIIB4 and, surprisingly, BIIB5-4scFv both demonstrated less than full (1:1) binding stoichiometry with hIGF-1R(1–903), suggesting geometric constraints within these BsAbs hindered the ability to engage all four binding arms.

Last, we developed a FRET assay to secondarily demonstrate the tetravalent, bispecific activity of BIIB4-5scFv, in particular because this BsAb was the only BsAb that did not have some form of impedance in the binding of all four of its binding arms (Fig. 3*C*). Using Europium-labeled BIIB4-5scFv and Cy5-labeled hIGF-1R(1–903), a robust FRET signal could be generated from the bound complex in solution. The FRET signal could be completely blocked using unlabeled BIIB4-5scFv. Combination of the BIIB4 and BIIB5 mAbs yielded a similar titration curve. However, the combination of the Fabs could only compete at an IC_{50} roughly 10-fold lower than that of the antibody combination and the BsAb, suggesting that having multiple IGF-1R recognition arms raises the apparent affinity in solution and that multivalency can be measured in the assay. Neither the BIIB4 mAb or Fab nor the BIIB5 mAb or Fab could bring the signal to baseline, indicating that both epitopes must be blocked simultaneously to inhibit BIIB4-5scFv from binding hIGF-1R(1–903). Consistent with the equilibrium SPR studies, the other BsAbs, 5scFv-BIIB4 and BIIB5-4scFv, could completely inhibit the FRET complex, however, at slightly reduced IC_{50} values (Fig. 3*D*). These results combined with the equilibrium SPR results indicate that only the BIIB4-5scFv BsAb has all its binding arms completely unimpeded for binding hIGF-1R.

Enhanced Ligand Blockade via Engagement of Two Inhibitory Epitopes—It was shown previously that combining the inhibitory antibody properties of both BIIB4 and BIIB5 leads to significantly enhanced inhibition of IGF-1R signaling and tumor cell growth, primarily due to enhanced ligand blockade (9). The goal of generating a BsAb targeting both inhibitory epitopes was to capture this activity within a single therapeutic candidate. Therefore, we assessed the ligand blocking properties of the various BsAbs to determine whether they could recapitulate what was observed with the BIIB4 and BIIB5 combination. The IGF-blocking ELISAs were designed to operate at concentrations near or above the affinity of the IGFs for IGF-1R, which enables the differentiation between allosteric and competitive mechanisms (8).

All the BsAbs were clearly superior to BIIB4 or BIIB5 in their ligand blocking capabilities (Fig. 4*A* (IGF-1 blocking) and *B* (IGF-2 blocking)). BIIB4-5scFv most effectively blocked IGF-1 and IGF-2 yielding a sharp inhibitory transition to baseline IGF binding levels with an IC_{50} near 1 nM. BIIB5-4scFv and 5scFv-BIIB4 also drove IGF binding to baseline levels, but with slightly broader transitions and IC_{50} values shifted out from that of BIIB4-5scFv, suggesting activity against both epitopes, but without the steep cooperative inhibition observed with BIIB4-5scFv. This result was repeated numerous times. Unlike the BsAbs, the tetravalent, BIIB5-5scFv, behaved similarly to the BIIB5 mAb with a marginal decrease in residual IGF binding at saturated BIIB5-5scFv levels.

Raising the level of IGF in the inhibitory ELISAs resulted in a decreased saturating level of blocking for allosteric inhibitors like BIIB5 and significantly reduced potency (IC_{50}) for competitive inhibitors like BIIB4, which must physically compete with ligand for binding the receptor (8). Based on the possibility that binding to the BIIB5 allosteric site may raise the effective concentration of the BsAb arms binding to the BIIB4 site, it was postulated that the BsAbs might not demonstrate the same IGF concentration-dependent decrease in activity that was observed for the mAbs. To test the hypothesis, inhibition curves using BIIB4, BIIB5, BIIB4 + BIIB5, and BIIB4-5scFv were generated using 250 nM IGF-1 in the inhibition assay (Fig. 4*C*). The inhibitory properties of BIIB4 and BIIB5 were clearly diminished at increased ligand levels as observed previously (8). Interestingly, the BIIB4-5scFv ligand blocking properties were unaffected by increasing IGF-1 levels 10-fold in the assay. The BIIB4 + BIIB5 mAb combination was also capable of completely inhibiting ligand at these elevated IGF-1 levels; however, the cooperativity of ligand blocking was visibly weaker (based on a broader inhibition curve) than what was observed with the BsAb. Similarly, no effect on the inhibitory properties of BIIB4-5scFv was observed when using 600 nM IGF-2 in the assay (data not shown).

Receptor Down-regulation—Antibody binding to IGF-1R can induce down-regulation of the receptor on cells. Previously, a possible correlation between the rate of down-regulation and the size of the immune complex (using soluble IGF-1R protein) formed by the engagement of an individual mAb or combination of mAbs was demonstrated (9).

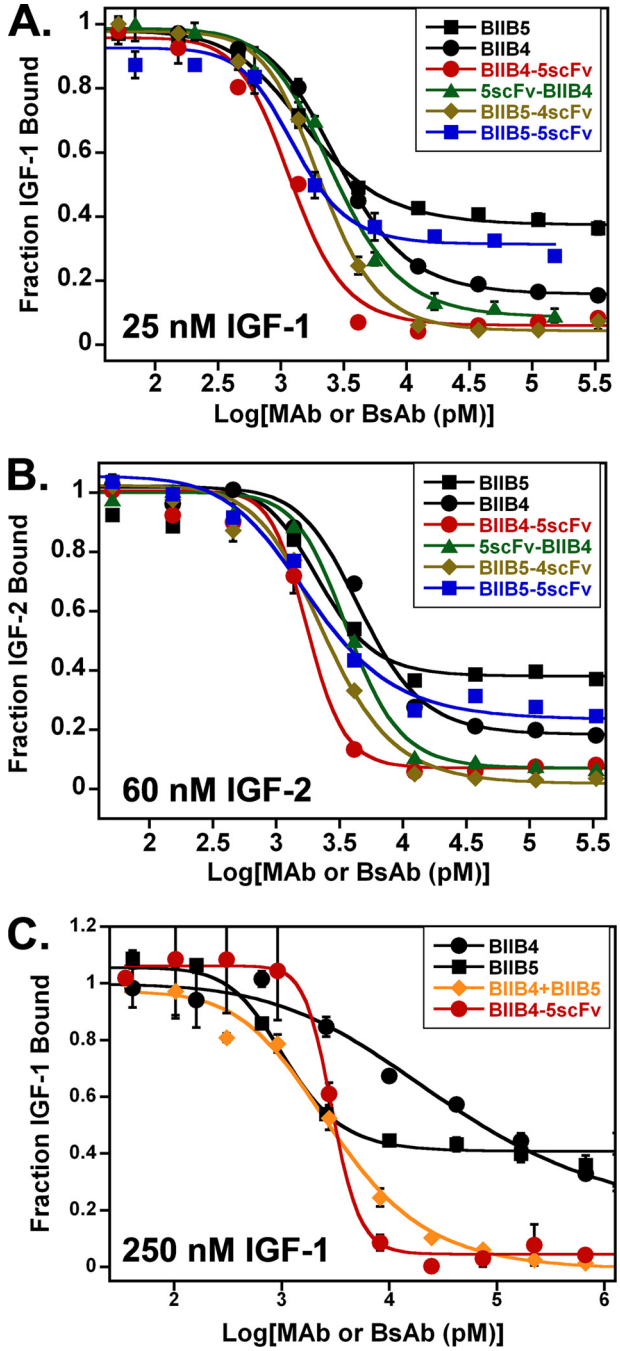

FIGURE 4. **Ligand blocking behavior of the mAbs and BsAbs.** *A* and *B*, mAb or BsAb blockade of a constant level of IGF-1 (25 nM, *A*) or IGF-2 (60 nM, *B*) binding to biotin-hIGF-1R-Fc. *C*, blockade of 250 nM IGF-1 by BIIB4, BIIB5, BIIB4 + BIIB5, and BIIB4-5scFv. For the BIIB4 + BIIB5 combination, the concentration on the *x* axis reflects the concentration of each of the mAbs and not the sum of their concentrations.

Here, the sizes of the soluble immune complexes formed between hIGF-1R(1–903) and BIIB4-5scFv or 5scFv-BIIB4 were determined using size exclusion chromatography with in-line static light scattering (Table 3). Complexes between hIGF-1R(1–903) and BIIB4, BIIB5, and the combination of BIIB4 and BIIB5 were also analyzed for comparison and added to Table 3.

The ability of BIIB4-5scFv and 5scFv-BIIB4 to induce receptor down-regulation in the non-small cell lung carcinoma

TABLE 3
Size of immune complexes formed between mAb or BsAb and hIGF-1R(1–903)

Sample	hIGF-1R(1–903) size	mAb or BsAb size	Complex size	Immune complex[a]
		kDa		
IGF-1R:BIIB4	310	150	840	2:2
IGF-1R:BIIB5	310	150	2400	5:5
IGF-1R:BIIB4-5scFv	310	210	1000	2:2
IGF-1R:5scFv-BIIB4	310	210	>5000[b]	>10:10
IGF-1R:BIIB4:BIIB5	310	150	>5000[b]	>8:8

[a] Assumes an equal number of antibodies *versus* hIGF-1R(1–903).
[b] Scattering above the upper range of the detector. The ternary IGF-1R:BIIB4:BIIB5 immune complex was closer to the void volume (*i.e.* higher molecular weight) than the IGF-1R:5scFv-BIIB4 immune complex.

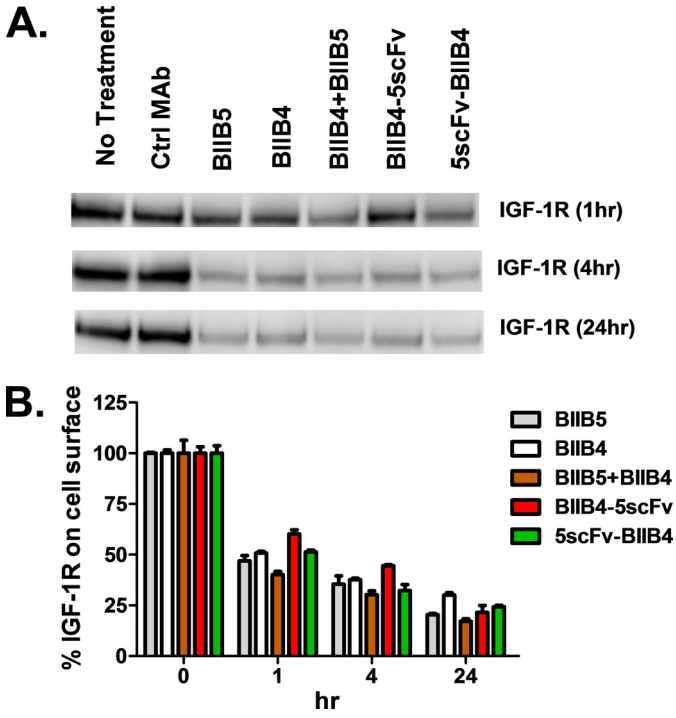

FIGURE 5. **IGF-1R down-regulation induced by the mAbs and BsAbs.** *A*, Western blot analyses of IGF-1R levels on human non-small cell lung carcinoma H322M cells following treatment with 100 nM BIIB4, BIIB5, BIIB4 + BIIB5, BIIB4-5scFv, or 5scFv-BIIB4. *B*, flow cytometric measurement of the level of IGF-1R on the surface of H322M cells subsequent to treatment with 100 nM BIIB4, BIIB5, BIIB4 + BIIB5, BIIB4-5scFv, or 5scFv-BIIB4. At 1 h, BIIB4-5scFv led to a reduced level of IGF-1R down-regulation compared with the BIIB4 + BIIB5 combination ($p < 0.02$) and 5scFv-BIIB4 ($p < 0.03$); however, given more time (24 h), BIIB4-5scFv was able to down-regulate the receptor to a similar degree.

line H322M was assessed by Western blot and flow cytometry. BIIB4-5scFv-induced receptor was slower than what was observed for BIIB4, BIIB5, or the BIIB4 + BIIB5 combination after treatment for 1 h (Fig. 5*A*). However, after incubation for 24 h, BIIB4-5scFv was able to degrade the receptor to a similar extent (Fig. 5*A*). A similar trend was observed for BIIB4-5scFv-induced IGF-1R internalization as analyzed by FACS measuring the relative percent of IGF-1R on the cell surface after treatment (Fig. 5*B*). In general, the size of the immune complex formed between the hIGF-1R(1–903) and the mAbs or BsAbs correlated with the observed rate of down-regulation; although the differences between these apparent rates was not substantial (*i.e.* not more than a 50% difference at 1 h).

Enhanced Inhibition of Tumor Cell Growth Activity in Vitro by the BsAbs—The ability of the BsAbs to inhibit tumor cell growth *in vitro* was assessed in several cell lines. First, the BIIB4-5scFv and 5scFv-BIIB4 BsAbs were tested for their ability to inhibit H322M cell growth in SFM driven by escalating levels of IGF-1 or IGF-2 (Fig. 6*A*). Interestingly, both BsAbs significantly reduced H322M cell growth over BIIB4 or BIIB5, particularly at high ligand concentrations. At the highest IGF-1 levels (0.3 and 1 μM), BIIB4-5scFv also demonstrated improved activity compared with the combination of BIIB4 and BIIB5, suggesting that the allosteric arm of the BsAb may significantly increase the effective concentration of the competitive binding arm, which results in an enhanced ability to block IGF-1 from binding the receptor (Fig. 6*A*). The same differentiation between BIIB4-5scFv and the BIIB4 + BIIB5 combination was not observed for IGF-2. The other BsAb, 5scFv-BIIB4, which is sterically hindered in its ability to engage all of its arms on IGF-1R, also showed superior activity compared with the single mAbs; however, the trend was that BIIB4-5scFv had the best activity (Fig. 6*A*).

Next, various BsAbs were titrated and assessed for their effects on H322M and osteosarcoma SJSA-1 tumor cell growth stimulated with a fixed level of IGF-1 (200 ng/ml). In this setup, all the BsAbs (BIIB4-5scFv, 5scFv-BIIB4, and BIIB5-4scFv) were superior to BIIB4 or BIIB5 at inhibiting H322M and SJSA-1 cell growth (Fig. 6, *B* and *C*). Consistent with other measures, BIIB4-5scFv tended to have the best activity of the BsAbs and slightly better activity than the BIIB4 + BIIB5 combination when titrated to lower concentrations (Fig. 6, *B* and *C*). Interestingly, the activity of the BIIB5-5scFv molecule, which contains four BIIB5 binding sites, was nearly identical to the BIIB5 mAb in the H322M assay, clearly demonstrating the importance of engaging both inhibitory epitopes for optimal activity (Fig. 6*B*).

Last, the cell growth inhibition properties of BIIB4-5scFv and 5scFv-BIIB4 were assessed in an increasing number of tumor cell lines using both IGF-1 and IGF-2 to stimulate growth. As observed in the previous assays, BIIB4-5scFv and 5scFv-BIIB4 were superior to the BIIB4 and BIIB5 mAbs at inhibiting IGF-1/2-driven tumor cell growth under serum-free conditions in H322M, BxPC3 (pancreas), A431 (skin), and A549 (lung) cell lines (Fig. 7*A*). As shown before, BIIB4-5scFv appeared to have slightly better growth inhibitory activity over both 5scFv-BIIB4 and the BIIB4 + BIIB5 combination. Similar results with the BsAbs were observed when assessing tumor cell growth inhibition stimulated by IGF-1 and IGF-2 in the presence of FBS in SJSA-1 and HT-29 (colon) cell lines (Fig. 7*B*) and in H322M, A549, BxPC3, and A431 cell lines (supplemental Fig. S3).

Disruption of IGF-1R-dependent Cellular Signaling and Activity by BIIB4-5scFv—The reduction of ligand-induced autophosphorylation of IGF-1R and the downstream phosphoinositide 3-kinase/Akt survival pathway by BIIB4-5scFv and mAb controls was determined using Western blot and plate-based assays. Western blot analyses demonstrate that treatment of SJSA-1 cells with BIIB4-5scFv resulted in significantly reduced IGF-1-dependent phosphorylation of both IGF-1R and Akt over BIIB4 or BIIB5, similar to what was ob-

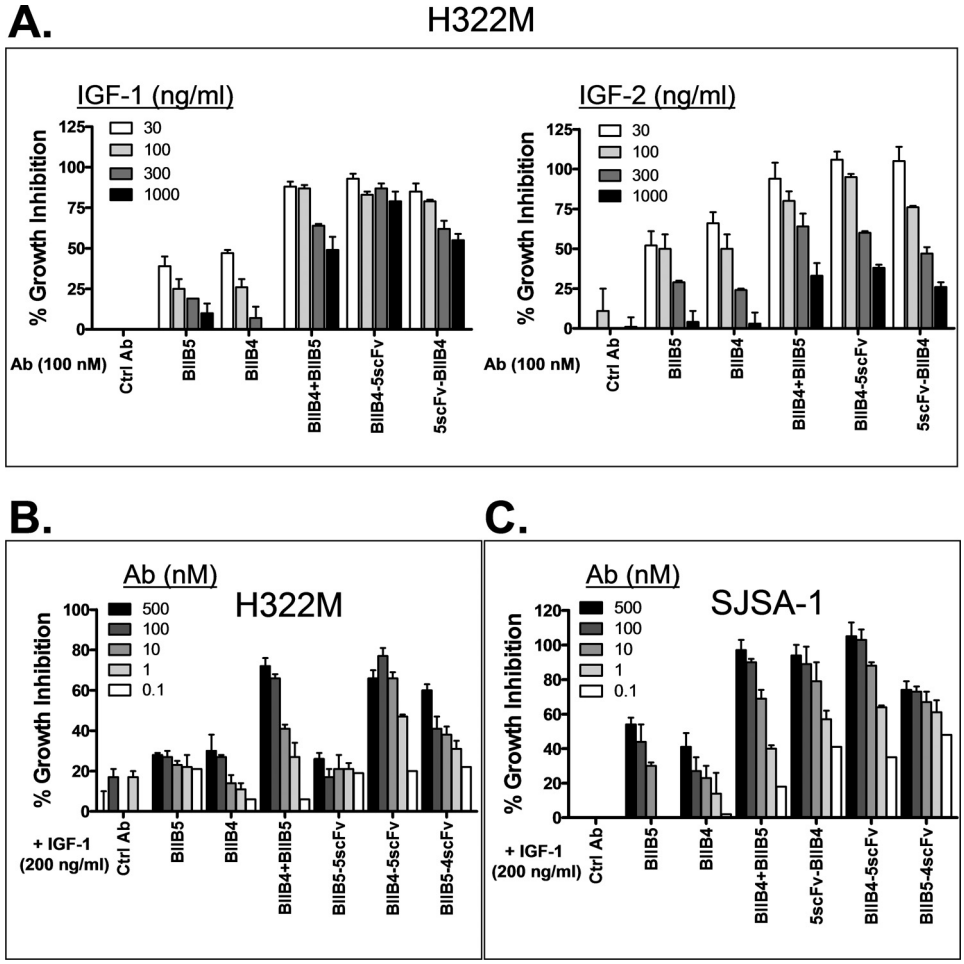

FIGURE 6. **Suppression of tumor cell growth at escalating IGF concentrations by mAbs and BsAbs.** *A,* human non-small cell lung carcinoma cell line H322M was subjected to escalating IGF-1 (*top left panel*) or IGF-2 (*top right panel*) in serum-free medium in the presence of 100 nM (from left to right) a control mAb, BIIB5, BIIB4, BIIB5 + BIIB4, BIIB4-5scFv, or 5scFv-BIIB4. H322M cells (*B*) or human osteosarcoma SJSA-1 cells (*C*) were subjected to 200 ng/ml of IGF-1-driven growth in SFM in the presence of titrating concentrations of mAbs or BsAbs.

served using the BIIB4 + BIIB5 combination (Fig. 8*A*). Meso Scale Discovery-based quantitative comparison of the ability of BIIB4, BIIB5, BIIB4 + BIIB5, and BIIB4-5scFv to inhibit IGF-1-stimulated Akt phosphorylation in SJSA-1, H322M, and A549 cells was performed. BIIB4-5scFv showed significantly improved inhibitory activity over BIIB4 and BIIB5 at all inhibitor concentrations in all three cell lines. BIIB4-5scFv showed marginal, but statistically significant ($p < 0.01$), improvement over BIIB4 + BIIB5 at 1 nM concentrations in SJSA-1 and A549 cells (Fig. 8, *B* and *D*).

The effect of BIIB4, BIIB5, the BIIB4 + BIIB5 combination, and BIIB4-5scFv on cell cycle progression and colony formation in soft agar of SJSA-1 cells was also assessed. The BIIB4 + BIIB5 combination and BIIB4-5scFv were able to completely reverse the effect of IGF stimulation by blocking tumor cell cycle progression into G_2/M phase and inducing cell cycle arrest in the G_0/G_1 phase to a degree similar to no IGF stimulation, whereas the BIIB4 and BIIB5 mAbs had a much weaker affect on IGF-induced progression toward mitosis (Fig. 9*A*). Additionally, treatment with the BIIB4 + BIIB5 combination or BIIB4-5scFv most significantly reduced the number of colonies formed by the SJSA-1 tumor cells in soft agar (Fig. 9*B*). This reduction was roughly 3-fold greater than what was observed when the cells were treated with BIIB4 or BIIB5 alone. Interestingly, addition of IGF-1 and IGF-2 partially reversed the inhibitory effect of BIIB4 and BIIB5, but not that of BIIB4-5scFv.

Pharmacokinetic Behavior of BsAbs—To test the PK behavior of BIIB4-5scFv and 5scFv-BIIB4 in comparison with BIIB4 and BIIB5 mAbs, all four proteins were dosed intraperitoneally in female adult nude mice. No significant difference was observed between the PK properties of the four molecules tested. The average half-life of the four test articles was 12.6 ± 2.3 days, and clearance (CL/F in ml/h/kg) was 0.26 ± 0.04 (Fig. 10*A*). A concern was that the ELISA used for detection of the BsAbs in serum was designed to detect IgG heavy chain and was insensitive to the presence of scFv. Thus, the presence of the scFv within both BIIB4-5scFv and 5scFv-BIIB4 in serum over time was assessed by Biacore solution, using the serum heavy chain concentrations determined by ELISA (supplemental Fig. 4, *A* and *B*). Sera containing BIIB4-5scFv and 5scFv-BIIB4 (whose scFvs are derived from the BIIB5 antibody) were tested for their ability to block BIIB5 binding to hIGF-1R(1–903) in the assay, which is sensitive to stoichiometry. Up to 7 days in serum, both BsAbs demonstrated the ability to completely block BIIB5 from binding

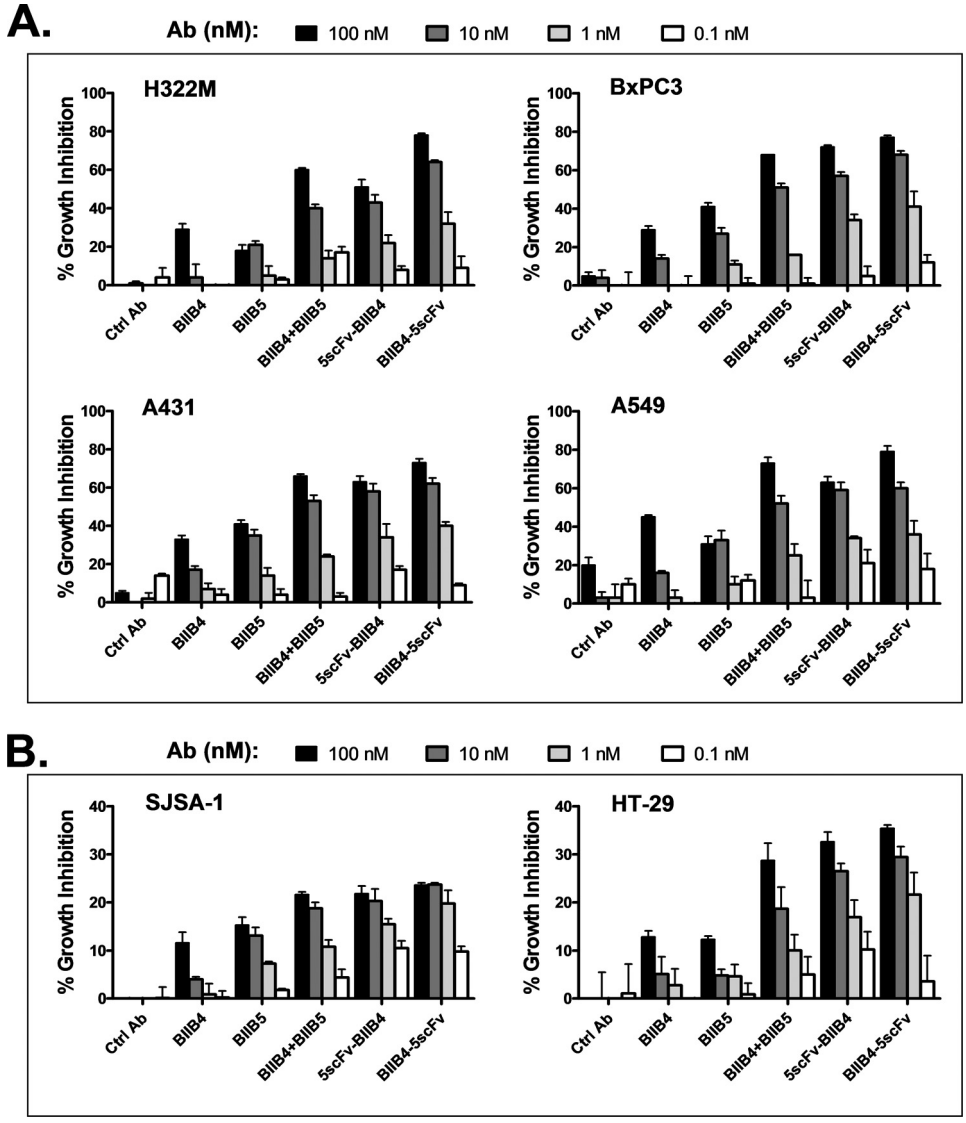

FIGURE 7. **Suppression of IGF-1 + IGF-2-driven tumor cell growth in multiple cell lines.** *A,* growth inhibition of human lung and pancreatic tumor cell lines in serum-free medium containing IGF-1 and IGF-2 (100 ng/ml each) in the presence of serial dilutions of the inhibitory mAbs or BsAbs. *B,* growth inhibition of SJSA-1 cells and human colon cancer HT-29 cells in 10% fetal bovine serum containing both IGF-1 and IGF-2 (200 ng/ml each) in the presence of serial dilutions of inhibitory mAbs or BsAbs.

hIGF-1R(1–903) at stoichiometries ±30% the expected level based on the concentrations determined using the heavy chain ELISA. Beyond 7 days, the concentration of BsAb in serum fell below the levels necessary for the assay. These data indicates the BsAbs are fully intact at least through 7 days in serum and likely beyond. Similar results were later confirmed in a second PK study using the Eu-labeled BIIB4-5scFv FRET assay.

In Vivo Efficacy of BIIB4-5scFv and 5scFv-BIIB4—Because IGF-1-driven growth, cell cycle progression, and colony formation of the SJSA-1 osteosarcoma cell line was much more sensitive to inhibition by BIIB4-5scFv than either BIIB4 or BIIB5 (Figs. 6*C*, 7*B*, and 9), this cell line was chosen for developing an *in vivo* tumor xenograft model to assess the activity of both BIIB4-5scFv and 5scFv-BIIB4 (which could not engage all its binding arms and was consistently less active than BIIB4-5scFv). Weekly dosing of mAbs and BsAbs began after size matching of the established SJSA-1 tumors, and the treatment continued for 3 weeks. The BIIB4-5scFv significantly reduced SJSA-1 tumor growth compared with the single mAbs and the 5scFv-BIIB4 BsAb (Fig. 10*B*). The efficacy study in this model was run two additional times, and the general result of BIIB4-5scFv yielding superior tumor growth inhibition over the mAbs was repeated each time. BIIB4-5scFv was also tested in other xenograft models, including HepG2 and H322M, and often a trend was observed that BIIB4-5scFv had improved activity (or at least equivalent activity) compared with BIIB4 or BIIB5; however, the data in these other models either did not repeat (as with H322M) or did not reach the level of statistical significance (HepG2).

DISCUSSION

Many strategies for utilizing BsAbs in oncology are being pursued. Perhaps the most common strategy involves the specific recruitment of immune effector cells, generally activated T cells, to tumor sites throughout the body (41, 42). More

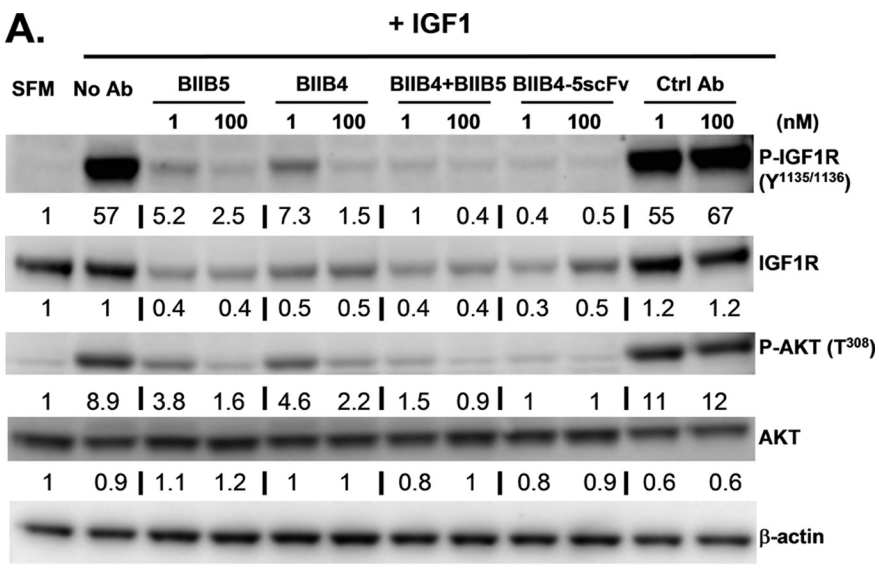
A.
+ IGF1
SFM
No Ab
BIIB5
BIIB4
BIIB4+BIIB5
BIIB4-5scFv
Ctrl Ab
1
100
(nM)
P-IGF1R (Y1135/1136)
1 57 5.2 2.5 7.3 1.5 1 0.4 0.4 0.5 55 67
IGF1R
1 1 0.4 0.4 0.5 0.5 0.4 0.4 0.3 0.5 1.2 1.2
P-AKT (T308)
1 8.9 3.8 1.6 4.6 2.2 1.5 0.9 1 1 11 12
AKT
1 0.9 1.1 1.2 1 1 0.8 1 0.8 0.9 0.6 0.6
β-actin

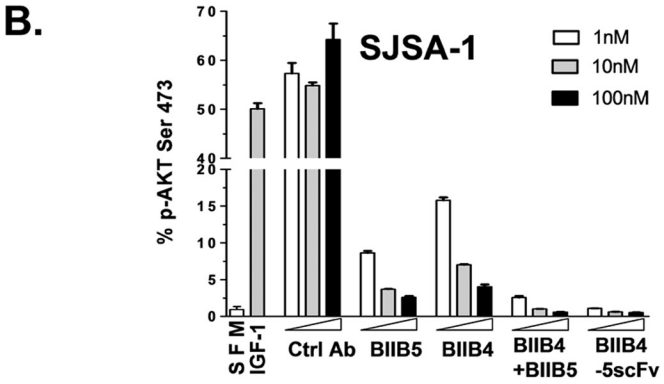
B.
SJSA-1
1nM
10nM
100nM
% p-AKT Ser 473
S F M
IGF-1
Ctrl Ab
BIIB5
BIIB4
BIIB4 +BIIB5
BIIB4 -5scFv

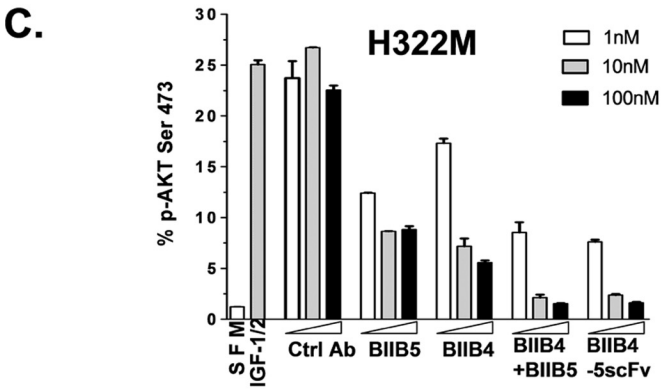
C.
H322M
1nM
10nM
100nM
% p-AKT Ser 473
S F M
IGF-1/2
Ctrl Ab
BIIB5
BIIB4
BIIB4 +BIIB5
BIIB4 -5scFv

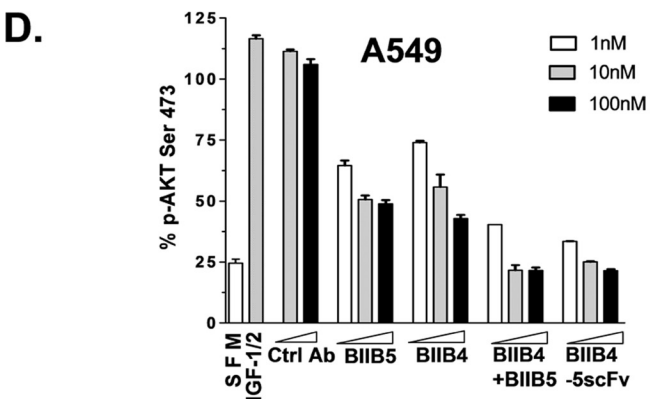
D.
A549
1nM
10nM
100nM
% p-AKT Ser 473
S F M
IGF-1/2
Ctrl Ab
BIIB5
BIIB4
BIIB4 +BIIB5
BIIB4 -5scFv

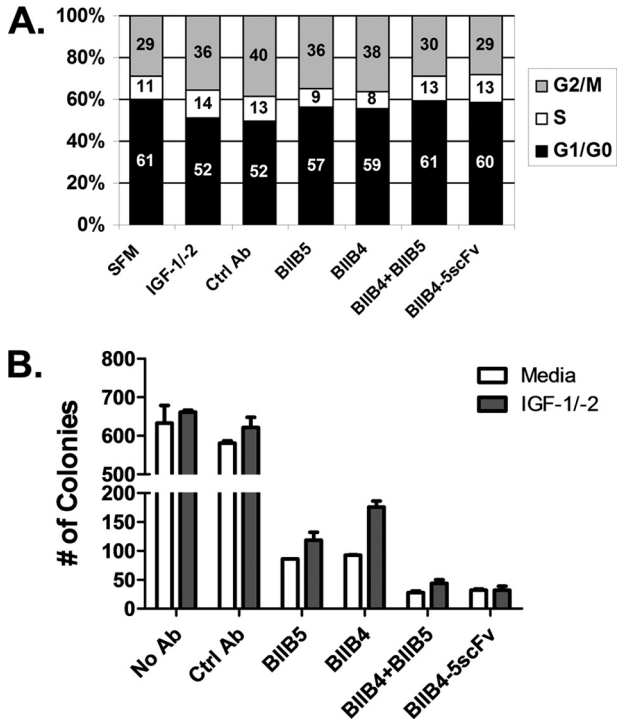

FIGURE 9. **Enhanced inhibitory effect of the BIIB4-5scFv BsAb on IGF-1/IGF-2-driven cell cycle progression and anchorage-independent cell growth of SJSA-1 cells.** *A,* the fraction of the cells in the G_1/G_0, S, and G_2/M cell cycles as characterized by FACS. Cells were cultured in SFM supplemented with 100 ng/ml of IGF-1 and IGF-2 and treated with 100 nM BIIB4, BIIB5, BIIB4 + BIIB5, or BIIB4-5scFv. *B,* the number of colonies formed in soft agar by SJSA-1 cells treated 100 nM BIIB4, BIIB5, BIIB4 + BIIB5, or BIIB4-5scFv in the absence or presence of IGF-1 and IGF-2 at 100 ng/ml each.

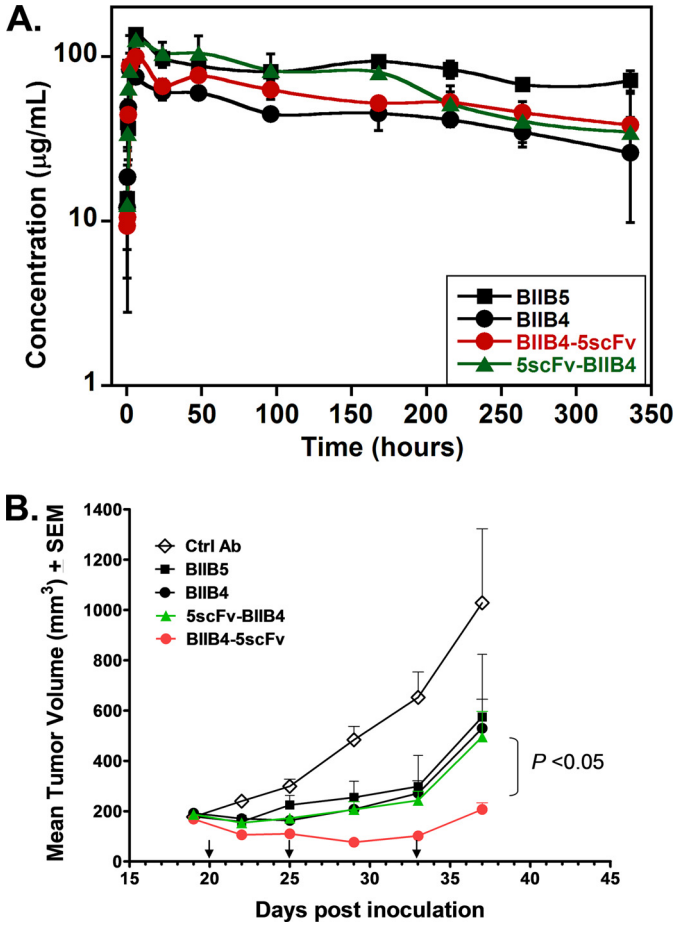

FIGURE 10. ***In vivo* pharmacokinetic and tumor regression results with BIIB4-5scFv and 5scFv-BIIB4.** *A,* serum concentrations of BIIB4, BIIB5, BIIB4-5scFv, and 5scFv-BIIB4 following 10 mg/kg of IP administration in female nude mice. *B,* growth of established SJSA-1 xenografts in female nude mice following intraperitoneal administration of equimolar doses of BIIB4 (7.5 mg/kg), BIIB5 (7.5 mg/kg), BIIB4-5scFv (10 mg/kg), and 5scFv-BIIB4 (10 mg/kg). *Arrows* pointing to the *x* axis indicate the days the mice were administered the test articles (three total). The doses were all at the saturating level of efficacy observed for each molecule. The differences in the tumor growth rate between the mAb treatment groups and the BIIB4-5scFv group were statistically significant (*, $p < 0.05$).

recent strategies have included the engagement of multiple cell surface receptors for either improved activation of tumor cell death machinery, such as TNFR family members (26), or the inhibition of multiple cell surface receptors responsible for cell survival, growth, angiogenesis, and metastases with the goal of overcoming acquired tumor resistance pathways (24, 43, 44).

Here, it was demonstrated that targeting multiple epitopes on a single receptor, IGF-1R in this case, can lead to a significant improvement over targeting a single epitope. We had previously demonstrated that combining the BIIB4 and BIIB5 mAbs led to a synergistic increase in the ability to shut down IGF-1R signaling beyond what could be achieved using saturating levels of the individual mAbs. In the BsAb format, the ability to target two epitopes led to an additional increase in the effective concentration of the antigen binding regions through avidity, which was likely the reason for the improved activity of BsAb over even the mAb combination at high levels of competing IGF-1. This was a property uniquely facilitated by the combination of an allosteric and competitive inhibitor into a single therapeutic. Targeting of multiple epitopes on a single antigen using a BsAb can have other advantages over the development of an antibody mixture. First, development of a single therapeutic is fundamentally less complex than the development of multiple drug products in a single vial or multiple vials from both a manufacturing and regulatory perspective. Combining a single target BsAb with other biologic therapies, which are all costly, would reduce the complexity and cost inherent if a combination were to include three biologics. Thus, there are various reasons why BsAbs that target a single antigen may have clinical utility both for efficacy and practical purposes.

Clinical development of BsAbs has been hindered for many reasons including general issues surrounding their manufacturability and physiochemical properties (22). Recombinantly derived bispecific designs, particularly those that include antibody fragments such as scFvs or single variable domains,

FIGURE 8. **Reduction of IGF-1R signaling and downstream Akt activation.** *A,* Western blot analyses of the phosphorylated and total protein levels of IGF-1R and Akt in SJSA-1 cells stimulated with IGF-1 in the presence or absence of BIIB4, BIIB5, BIIB4 + BIIB5, or BIIB4-5scFv. The *numbers under* the blots are the relative densitometric readings for each band. *B–D,* Meso Scale Discovery analyses of the affects of BIIB4, BIIB5, BIIB4 + BIIB5, or BIIB4-5scFv on IGF-1-mediated Akt phosphorylation in SJSA-1 cells (*B*), and IGF-1/IGF-2-mediated Akt phosphorylation in H322M (*C*), and A549 (*D*) tumor cells.

taken out of their native IgG context have been fraught with instability, expression, and aggregation issues. There are a few reports of such issues (23, 24), and many cases that do not get reported. Managing the physiochemical properties during the design of novel antibody-like or BsAb constructs has been an important part of their successful design for clinical purposes (45–48). We have found that including a stabilization step for scFvs has resulted in a general methodology for generating IgG-like BsAbs with sufficient stability and solubility for development (25, 26). By taking the approach of stabilizing each scFv used within a BsAb instead of choosing antibodies or scFvs based on their stability, the choice of antibodies to be used within a BsAb can rest on their activity.

Subsequent to the scFv stabilization step (supplemental Fig. S1), two of the BsAbs described here, 5scFv-BIIB4 and BIIB4-5scFv, were scaled to yield over 1 g of material, and research cell lines could be rapidly developed to express over 100 mg/liter of protein. Amplification led to production cell lines with titers as high as 3.7 g/liter for BIIB4-5scFv, which is more than acceptable for a commercial cell line. Additionally, these constructs could be maintained for months under refrigeration at concentrations >5 mg/ml with no issues and no special formulations. With methodologies in place to produce BsAbs with ideal biophysical properties, we expect a general increase in the investigation of BsAbs in clinical trials over the next few years.

An interesting feature of the IgG-like BsAb format described here is the ability to screen multiple BsAb constructs with varying antigen binding geometries. The goal was to generate a single BsAb with equivalent or better activity compared with the synergistic BIIB4 + BIIB5 mAb combination that was described previously (9). The importance of testing the various BsAb geometries was evident in that only one format, BIIB4-5scFv, had equivalent or better activity than the BIIB4 + BIIB5 combination. Spacing the antigen binding domains of the BsAb by appending the BIIB5 scFv to the C terminus had a clear advantage over the N-terminal format where the two binding regions were more closely positioned. For 5scFv-BIIB4 (N-terminal scFvs), binding of either the BIIB4 or BIIB5 epitopes was impeded by engagement of the other epitope. We also observed a similar result with N- and C-terminal BsAbs in a different system, where the N-terminal BsAb clearly could not engage its two epitopes fully (26). An unexpected finding was that BIIB5-4scFv was less active than BIIB4-5scFv. Appending BIIB4 scFvs to the C termini of an IgG did not result in an ability to fully engage both scFvs on IGF-1R as was observed with BIIB4-5scFv. Thus, the ability to explore multiple geometries and multiple scFvs clearly enabled us to find a format that led to optimal inhibition of IGF-1R signaling. It will be interesting to observe the extent to which similar testing of various antigen binding geometries is necessary for obtaining ideal bispecific activity within other IgG-like BsAb formats (44, 49, 50).

Although the murine *in vivo* data with the SJSA-1 model demonstrated improved tumor growth inhibition for BIIB4-5scFv over single mAbs in three independent studies, such robust results were not apparent in the other models that were tested. The H322M tumor model was run twice. Once BIIB5-4scFv showed remarkably improved activity over single mAbs, but this did not repeat in a second study. The HepG2 model was also run twice, and the BIIB4-5scFv was always the most efficacious molecule at saturating doses, but the difference between it and the most potent single mAb in each study (which varied) was marginal and did not achieve statistical significance. It is possible that H322M and HepG2 tumors rely heavily on multiple growth and survival pathways and improved inhibition in IGF-1R signaling alone is difficult to measure in this limited window of efficacy afforded by IGF-1R therapy. One potential advantage of BIIB4-5scFv that could not be tested using the *in vivo* murine xenograft models was its comparative efficacy at elevated levels of IGF-1, where the *in vitro* data showed a distinct advantage for the BsAb. This scenario may be highly relevant in human patients because elevated levels of IGF-1 are commonly associated with anti-IGF-1R mAb treatment (51). Recapitulating this aspect of anti-IGF-1R treatment in mice is difficult due to the lack of cross-reactivity of the test articles to mouse IGF-1R.

Last, the study described here also enabled us to evaluate the relative importance of ligand blocking and receptor down-regulation on IGF-1R signaling and IGF-1R-dependent cell growth. Unlike the BIIB4 and BIIB5 mAbs, BIIB4-5scFv was capable of completely inhibiting any association of IGF-1R with either IGF-1 or IGF-2 regardless of the ligand concentrations. This result was recapitulated in the cellular proliferation assays performed under artificially high IGF-1 concentrations, a potentially important scenario that can be induced by many anti-IGF-1R inhibitors. Surprisingly, elevated IGF-2 levels did reduce the activity of BIIB4-5scFv (although not to as significant an extent as was observed for BIIB4 or BIIB5). We found that BIIB4-5scFv biochemically blocks IGF-2 from binding IGF-1R even at highly elevated ligand concentrations. It is possible that high IGF-2 activity in the cell proliferation assays may be due to IGF-2 binding to IR, and not a competition with BIIB4-scFv for IGF-1R (52). Last, BIIB4-5scFv was not superior to the mAbs in its ability to down-regulate IGF-1R. We therefore surmise that the enhanced activity of the BsAb was due to its ability to more effectively abrogate IGF-1R interaction with its ligands.

Acknowledgments—We gratefully acknowledge Drs. Kristin Demarest and Simon Watkins for critical reading of the manuscript.

REFERENCES

1. Fedi, P., Kimmelman, A., and Aaronson, S. A. (2000) in *Holland-Frei Cancer Medicine* (Bast, R. C., Kufe, D. W., Pollock, R. E., Weichselbaum, R. R., Holland, J. F., and Frei, E., eds) 5th Ed., pp. 33–55, People's Medical Publishing House-U.S.A., Shelton, CT
2. Pollak, M. N., Schernhammer, E. S., and Hankinson, S. E. (2004) *Nat. Rev. Cancer* **4,** 505–518
3. Arteaga, C. L., Kitten, L. J., Coronado, E. B., Jacobs, S., Kull, F. C., Jr., Allred, D. C., and Osborne, C. K. (1989) *J. Clin. Invest.* **84,** 1418–1423
4. Jacobs, S., Cook, S., Svoboda, M. E., and Van Wyk, J. J. (1986) *Endocrinology* **118,** 223–226
5. Pollak, M. (2008) *Curr. Opin. Pharmacol.* **8,** 384–392
6. Hewish, M., Chau, I., and Cunningham, D. (2009) *Recent Pat. Anticancer Drug Discov.* **4,** 54–72
7. Soos, M. A., Field, C. E., Lammers, R., Ullrich, A., Zhang, B., Roth, R. A.,

Andersen, A. S., Kjeldsen, T., and Siddle, K. (1992) *J. Biol. Chem.* **267,** 12955–12963
8. Doern, A., Cao, X., Sereno, A., Reyes, C. L., Altshuler, A., Huang, F., Hession, C., Flavier, A., Favis, M., Tran, H., Ailor, E., Levesque, M., Murphy, T., Berquist, L., Tamraz, S., Snipas, T., Garber, E., Shestowsky, W. S., Rennard, R., Graff, C. P., Wu, X., Snyder, W., Cole, L., Gregson, D., Shields, M., Ho, S. N., Reff, M. E., Glaser, S. M., Dong, J., Demarest, S. J. and Hariharan, K. (2009) *J. Biol. Chem.* **284,** 10254–10267
9. Dong, J., Demarest, S. J., Sereno, A., Tamraz, S., Langley, E., Doern, A., Snipas, T., Perron, K., Joseph, I., Glaser, S. M., Ho, S. N., Reff, M. E., and Hariharan, K. (2010) *Mol. Cancer Ther.* **9,** 2593–2605
10. Pedersen, M. W., Jacobsen, H. J., Koefoed, K., Hey, A., Pyke, C., Haurum, J. S., and Kragh, M. (2010) *Cancer Res.* **70,** 588–597
11. Scheuer, W., Friess, T., Burtscher, H., Bossenmaier, B., Endl, J., and Hasmann, M. (2009) *Cancer Res.* **69,** 9330–9336
12. van der Horst, E. H., Chinn, L., Wang, M., Velilla, T., Tran, H., Madrona, Y., Lam, A., Ji, M., Hoey, T. C., and Sato, A. K. (2009) *Neoplasia* **11,** 355–364
13. Cheng, L. W., Stanker, L. H., Henderson, T. D., 2nd, Lou, J., and Marks, J. D. (2009) *Infect. Immun.* **77,** 4305–4313
14. Demarest, S. J., Hariharan, M., Elia, M., Salbato, J., Jin, P., Bird, C., Short, J. M., Kimmel, B. E., Dudley, M., Woodnutt, G., and Hansen, G. (2010) *mAbs* **2,** 190–198
15. Fischer, N., and Léger, O. (2007) *Pathobiology* **74,** 3–14
16. Staerz, U. D., and Bevan, M. J. (1986) *Proc. Natl. Acad. Sci. U.S.A.* **83,** 1453–1457
17. Glennie, M. J., McBride, H. M., Worth, A. T., and Stevenson, G. T. (1987) *J. Immunol.* **139,** 2367–2375
18. Heiss, M. M., Murawa, P., Koralewski, P., Kutarska, E., Kolesnik, O. O., Ivanchenko, V. V., Dudnichenko, A. S., Aleknaviciene, B., Razbadauskas, A., Gore, M., Ganea-Motan, E., Ciuleanu, T., Wimberger, P., Schmittel, A., Schmalfeldt, B., Burges, A., Bokemeyer, C., Lindhofer, H., Lahr, A., and Parsons, S. L. (2010) *Int. J. Cancer,* doi 10.1002/ijc. 25423
19. Kontermann, R. E. (2010) *Curr. Opin. Mol. Ther.* **12,** 176–183
20. Coloma, M. J., and Morrison, S. L. (1997) *Nat. Biotechnol.* **15,** 159–163
21. Chan, A. C., and Carter, P. J. (2010) *Nat. Rev. Immunol.* **10,** 301–316
22. Demarest, S. J., and Glaser, S. M. (2008) *Curr. Opin. Drug Discov. Devel.* **11,** 675–687
23. Qu, Z., Goldenberg, D. M., Cardillo, T. M., Shi, V., Hansen, H. J., and Chang, C. H. (2008) *Blood* **111,** 2211–2219
24. Lu, D., Zhang, H., Koo, H., Tonra, J., Balderes, P., Prewett, M., Corcoran, E., Mangalampalli, V., Bassi, R., Anselma, D., Patel, D., Kang, X., Ludwig, D. L., Hicklin, D. J., Bohlen, P., Witte, L., and Zhu, Z. (2005) *J. Biol. Chem.* **280,** 19665–19672
25. Miller, B. R., Demarest, S. J., Lugovskoy, A., Huang, F., Wu, X., Snyder, W. B., Croner, L. J., Wang, N., Amatucci, A., Michaelson, J. S., and Glaser, S. M. (2010) *Protein Eng. Des. Sel.* **23,** 549–557
26. Michaelson, J. S., Demarest, S. J., Miller, B., Amatucci, A., Snyder, W. B., Wu, X., Huang, F., Phan, S., Gao, S., Doern, A., Farrington, G. K., Lugovskoy, A., Joseph, I., Bailly, V., Wang, X., Garber, E., Browning, J., and Glaser, S. M. (2009) *mAbs* **1,** 128–141
27. Miller, B. R., Glaser, S. M., and Demarest, S. J. (2009) *Methods Mol. Biol.* **525,** 279–289
28. Garber, E., and Demarest, S. J. (2007) *Biochem. Biophys. Res. Commun.* **355,** 751–757
29. Wang, N., Smith, W. F., Miller, B. R., Aivazian, D., Lugovskoy, A. A., Reff, M. E., Glaser, S. M., Croner, L. J., and Demarest, S. J. (2009) *Proteins* **76,** 99–114
30. Jordan, J. L., Arndt, J. W., Hanf, K., Li, G., Hall, J., Demarest, S., Huang, F., Wu, X., Miller, B., Glaser, S., Fernandez, E. J., Wang, D., and Lugovskoy, A. (2009) *Proteins* **77,** 832–841
31. Urlaub, G., Käs, E., Carothers, A. M., and Chasin, L. A. (1983) *Cell* **33,** 405–412
32. Majors, B. S., Betenbaugh, M. J., Pederson, N. E., and Chiang, G. G. (2008) *Biotechnol. Bioeng.* **101,** 567–578
33. Majors, B. S., Arden, N., Oyler, G. A., Chiang, G. G., Pederson, N. E., and Betenbaugh, M. J. (2008) *J. Biotechnol.* **138,** 103–106
34. Brezinsky, S. C., Chiang, G. G., Szilvasi, A., Mohan, S., Shapiro, R. I., MacLean, A., Sisk, W., and Thill, G. (2003) *J. Immunol. Methods* **277,** 141–155
35. Day, E. S., Cachero, T. G., Qian, F., Sun, Y., Wen, D., Pelletier, M., Hsu, Y. M., and Whitty, A. (2005) *Biochemistry* **44,** 1919–1931
36. Wörn, A., and Plückthun, A. (2001) *J. Mol. Biol.* **305,** 989–1010
37. Taylor, F. R., Prentice, H. L., Garber, E. A., Fajardo, H. A., Vasilyeva, E., and Pepinsky, R. B. (2006) *Anal. Biochem.* **353,** 204–208
38. Demarest, S. J., Chen, G., Kimmel, B. E., Gustafson, D., Wu, J., Salbato, J., Poland, J., Elia, M., Tan, X., Wong, K., Short, J., and Hansen, G. (2006) *Protein Eng. Des. Sel.* **19,** 325–336
39. Röthlisberger, D., Honegger, A., and Plückthun, A. (2005) *J. Mol. Biol.* **347,** 773–389
40. Hoet, R. M., Cohen, E. H., Kent, R. B., Rookey, K., Schoonbroodt, S., Hogan, S., Rem, L., Frans, N., Daukandt, M., Pieters, H., van Hegelsom, R., Neer, N. C., Nastri, H. G., Rondon, I. J., Leeds, J. A., Hufton, S. E., Huang, L., Kashin, I., Devlin, M., Kuang, G., Steukers, M., Viswanathan, M., Nixon, A. E., Sexton, D. J., Hoogenboom, H. R., and Ladner, R. C. (2005) *Nat. Biotechnol.* **23,** 344–348
41. Müller, D., and Kontermann, R. E. (2007) *Curr. Opin. Mol. Ther.* **9,** 319–326
42. Bargou, R., Leo, E., Zugmaier, G., Klinger, M., Goebeler, M., Knop, S., Noppeney, R., Viardot, A., Hess, G., Schuler, M., Einsele, H., Brandl, C., Wolf, A., Kirchinger, P., Klappers, P., Schmidt, M., Riethmüller, G., Reinhardt, C., Baeuerle, P. A., and Kufer, P. (2008) *Science* **321,** 974–977
43. Robinson, M. K., Hodge, K. M., Horak, E., Sundberg, A. L., Russeva, M., Shaller, C. C., von Mehren, M., Shchaveleva, I., Simmons, H. H., Marks, J. D., and Adams, G. P. (2008) *Br. J. Cancer* **99,** 1415–1425
44. Bostrom, J., Yu, S. F., Kan, D., Appleton, B. A., Lee, C. V., Billeci, K., Man, W., Peale, F., Ross, S., Wiesmann, C., and Fuh, G. (2009) *Science* **323,** 1610–1614
45. Willuda, J., Honegger, A., Waibel, R., Schubiger, P. A., Stahel, R., Zangemeister-Wittke, U., and Plückthun, A. (1999) *Cancer Res.* **59,** 5758–5767
46. Pastan, I., Hassan, R., Fitzgerald, D. J., and Kreitman, R. J. (2006) *Nat. Rev. Cancer* **6,** 559–565
47. Famm, K., Hansen, L., Christ, D., and Winter, G. (2008) *J. Mol. Biol.* **376,** 926–931
48. Barthelemy, P. A., Raab, H., Appleton, B. A., Bond, C. J., Wu, P., Wiesmann, C., and Sidhu, S. S. (2008) *J. Biol. Chem.* **283,** 3639–3654
49. Wu, C., Ying, H., Grinnell, C., Bryant, S., Miller, R., Clabbers, A., Bose, S., McCarthy, D., Zhu, R. R., Santora, L., Davis-Taber, R., Kunes, Y., Fung, E., Schwartz, A., Sakorafas, P., Gu, J., Tarcsa, E., Murtaza, A., and Ghayur, T. (2007) *Nat. Biotechnol.* **25,** 1290–1297
50. Dimasi, N., Gao, C., Fleming, R., Woods, R. M., Yao, X. T., Shirinian, L., Kiener, P. A., and Wu, H. (2009) *J. Mol. Biol.* **393,** 672–692
51. Pollak, M. (2008) *Nat. Rev. Cancer* **8,** 915–928
52. Frasca, F., Pandini, G., Scalia, P., Sciacca, L., Mineo, R., Costantino, A., Goldfine, I. D., Belfiore, A., and Vigneri, R. (1999) *Mol. Cell. Biol.* **19,** 3278–3288